Adaptive Control of Nonlinear Systems with Input Loss of Effectiveness, Saturation, and Friction

D.J. López-Araujo[1], A. Loría[2], N. Alvarez-Jarquin[1], J. Morales-Morales[3], J. Sosa-Herrera[†]

Abstract— **We address the tracking control problem of second-order systems under the effect of friction, faults, and saturation, which are inherent to most physical systems. Our main contribution is an adaptive controller that ensures convergence of the tracking errors despite input loss of effectiveness. The designed control explicitly considers the system maximum admitted input, effectively preventing saturation during operation. Additionally, the controller incorporates viscous and Coulomb friction terms. By integrating these features, the controller maintains robustness even under conditions where parameter uncertainty or input limitations would otherwise degrade performance. The stability of the closed-loop system is analyzed using Lyapunov's theory, achieving demonstrating uniform global stability and convergence of the tracking error. The effectiveness of the proposed controller is further validated through simulations, demonstrating its capability to maintain stable performance despite the real-word considerations made.**

I. INTRODUCTION

Motivation. To guarantee efficient operation, real-life systems must meet high standards of reliability and safety. To achieve these requirements, control techniques must account for physical phenomena affecting system behavior in real-world scenarios. For instance, undesirable effects may appear when control commands exceed the capabilities actuators are able to provide, leading to input saturation. Driving the actuator beyond its intended operation range may cause increased power consumption, decreased performance, and a shortened actuator lifespan, among other issues [1]. Another common actuator related issue is loss of effectiveness; in which the effectively provided input is reduced in comparison to that calculated by the control algorithm. If the loss is significant, this phenomenon degrade performance and may compromise stability. Additionally, friction must be considered, as it can introduce undesirable behavior, particularly when operating at low velocities due to the Stribeck effect [2], [3]. Dry friction can cause abrupt starts, poor response, or even stall the actuator if the applied force fails to surpass the friction level. The Coulomb component of dry friction, on the other hand, can cause variations in the actuator speed, degrading the system's accuracy and stability, potentially leading to stick-slip motion [4].

[1] López-Araujo D. J. and Alvarez-Jarquin N. are with SECIHTI, CentroGeo, Circuito Tecnopolo Norte 117, 20313, Aguascalientes, Mexico, Sosa-Herrera J. (deceased) was also with SECIHTI, CentroGeo, djlopez/nalvarez@centrogeo.edu.mx

[2] Loría A. is with L2S, CNRS, 3 Rue Joliot Curie, Gif sur Yvette, France, antonio.loriar@cnrs.fr

[3] Morales-Morales J. is with is with UASLP, Región Altiplano, Carretera Cedral km 5+600, Matehuala, 78700, San Luis Potosí, Mexico, josefa.morales@uaslp.mx

Literature review and open problems. One of the key challenges to compensate the friction effects is that being a highly non-linear and uncertain phenomenon is difficult to model. For instance, an approach using the LuGre friction model compensates the undesired effects with dynamic surface control [5]; later in [6] a data-driven strategy was adopted by integrating sliding mode control with neural network to improve the system performance. Adaptive control strategies based on continuous friction models have been proposed, *e.g.* in [7], [8], [9], [10]. The introduced smooth friction models, simplify the Lyapunov stability analysis, as they avoid discontinuities and ensure that the system dynamics is well-defined. In this context, adaptive parameter estimation schemes that adjust to changes in the system dynamics, including frictional effects, were developed [9], [10]. Both the robust integral of the sign of the error (RISE) feedback term, as well as the neural network approximation, strength system robustness against modeling uncertainties and external disturbances.

Nevertheless, in most of the works mentioned above it is assumed that the actuator is able to deliver any control input computed by the controller. In practice, actuators operation range is restricted, demanding beyond this limit leads to input saturation, which can affect performance and stability. Only few studies address saturation explicitly while also considering friction effects. For instance, robotic manipulators with non-linear static friction and input saturation were studied in [11] and [12], achieving semi-global stabilization via adaptive control. However, one limitation of semi-global stability within a bounded input framework, is that while the region of attraction can be expanded by adjusting the control gains, if the gains are set too high, they may cause the actuator to reach their saturation value. In addition, actuators may suffer from loss of effectiveness, this effect differ from input saturation, as the control input is attenuated rather than reaching hard bounds. Existing works provide some solutions based on different control approaches, for instance [13] and [14] address parametric uncertainties and nonlinearities in electro-hydraulic systems combining backstepping with adaptive control, but only few simultaneously consider friction, loss of effectiveness, and actuator saturation.

Contributions. To overcome the problems mentioned above, the developed work presents analytical tools that ensure the tracking control objective is achieved globally while maintaining system performance in the case of a loss of effectiveness. As far as the authors are aware, no other work guarantees uniform global stability while addressing input failure, input saturation, and viscous and static friction in the dynamics. This paper tailors an adaptive control methodology (developed for robot manipulators with unknown parameters [15]) to address input failure, specifically loss of effectiveness. For simplicity, our analysis focuses on 1 dof systems, but it may be extended to multivariable systems. The proposed control method accounts for input saturation and friction, ensuring that the actuator signal stays within its prescribed limits.

The paper is organized as follows: In Section II we provide a precise problem statement. Our main results are presented in Section III, and we provide some illustrative simulation examples in Section IV before concluding with some remarks.

II. Problem formulation

A. The plant model

Let us consider an actuation element modeled as a spring-damper system under the influence of both Coulomb and viscous friction. Electro-magnetic, pneumatic, and other types of actuation can be represented by a similar model [16], [17]. The motion of the system can be described by the following equation:

$$\tau = m\ddot{x} + f_v\dot{x} + f_c \tanh(\beta\dot{x}) + \alpha g(x) \tag{1}$$

where $m > 0$ represents the moving mass, $f_v > 0$ and $f_c > 0$ are the damping coefficients associated with viscous and Coulomb friction, respectively, β is a parameter that defines the tolerance for velocity variations, $\alpha g(x)$ represents the restorative force term, where $\alpha > 0$ and $g : \mathbb{R} \to \mathbb{R}$. The function g may take different forms depending on the system under consideration. For instance, $g(x) = x$ for a 3-element pneumatic-muscle system, whereas $g(x) = \sin(x)$ for an actuated simple pendulum.

The viscous friction component f_v is proportional to the velocity $\dot{x}$, representing the resistance to motion that increases with speed. In contrast, the term involving Coulomb friction, $f_c \tanh(\beta\dot{x})$, models the static friction component that must be overcome to initiate movement. This smooth Coulomb friction model, which uses the hyperbolic tangent function $\tanh(\cdot)$, is selected specifically to avoid the discontinuities typically introduced by more conventional dry friction models, which can make the analysis and control design more challenging. In [18], a smooth model using $\tanh(\beta\dot{x})$ was reported to emulate discontinuous friction under certain conditions.

The smoothness introduced by $\tanh(\beta\dot{x})$ provides a gradual transition as the system moves from static to dynamic friction states, which is advantageous for the theoretical analysis and the practical applications [7], [19]. To ensure the desired boundedness of the proposed control law, the following assumption is essential.

Assumption 1: The restoring force term $\alpha g(x)$ is known and bounded for all $t \in \mathbb{R}_+$, *i.e.,* there exists a positive constant B_{RF} such that $|\alpha g(x)| \leq B_{RF}$ for all $t \in \mathbb{R}_+$. □

Assumption 1 is not conservative; it is satisfied by many practical systems. For instance, magnetic actuators often exhibit saturation effects [20], where the force increases with displacement until it reaches a maximum value. This results in a naturally bounded restoring force.

B. Unknown parameters

It is assumed that m, f_v, f_c, and α in (1) are unknown. For the sequel, these are generically referred to as θ_j^*, with $j \in \{1, \ldots, 4\}$, then we assume the following:

Assumption 2: The unknown parameter θ_j^* satisfies

$$|\theta_j^*| < B_{aj} \quad \forall j \in \{1, 2, 3, 4\} \tag{2}$$

where B_{aj} are known. □

For the sequel, we define $\theta^* \triangleq \begin{bmatrix}\theta_1^* \cdots \theta_4^*\end{bmatrix}^\top$, $B_a \triangleq \begin{bmatrix}B_{a1} \cdots B_{a4}\end{bmatrix}^\top$ and $\Theta \triangleq [-B_{a1}, B_{a1}] \times \cdots \times [-B_{a4}, B_{a4}]$. Hence, we have $\theta^* \in \Theta$.

Property 1: The system dynamics are linear with respect to parameters; *i.e.,* they can be expressed as

$$m\ddot{x} + f_v\dot{x} + f_c \tanh(\beta\dot{x}) + \alpha g(x) = \Upsilon(x, \dot{x}, \ddot{x})^\top \theta^*$$

where $\Upsilon : \mathbb{R} \to \mathbb{R}^4$ is a known regressor function. □

C. Input fault and input saturation

It is assumed that the actuators are affected by a loss of effectiveness, which may be modeled using a piecewise constant function $\Delta : \mathbb{R}_+ \to (\delta_m, 1]$, with $\delta_m \in (0, 1]$. More precisely, it is assumed that the actual control torque τ in (1) corresponds to

$$\tau = \Delta(t)u$$

where u represents the computed control input. Thus, u is known, while Δ is not. However, we assume the following.

Assumption 3: The loss-of-effectiveness function $t \mapsto \Delta$ is piecewise constant on the intervals $t \in (t_k, t_{k+1}]$. Moreover, the jump discontinuities at the points t_k are uniformly bounded, *i.e.*, there exists $c > 0$ such that

$$|\Delta(t_{k^+}) - \Delta(t_{k^-})| \leq c \quad \forall k$$

Additionally, there exists a minimum inter-event time $\tau_d > 0$ such that

$$t_{k+1} - t_k \geq \tau_d \quad \forall k$$

□

To prevent the control input from exceeding the saturation limits of the actuator, its natural real-life limits are modeled through a saturation constraint *i.e.,* $|\tau| \leq T$, where $T > 0$ stands for the maximum admissible actuator output. Accordingly, the control input is defined as

$$\tau(t) = T\text{sat}\left(\frac{\Delta(t)u}{T}\right) \tag{3}$$

where $\text{sat}(s) = \text{sign}(s)\min\{|s|, 1\}$.

Under the conditions described above, we address the problem of designing a state-feedback control law u, such that, defining the position $\bar{x} \triangleq x - x_d$ and tracking errors $\dot{\bar{x}} \triangleq \dot{x} - \dot{x}_d$ we have

$$\lim_{t\to\infty} \bar{x}(t) = 0 \qquad \lim_{t\to\infty} \dot{\bar{x}}(t) = 0$$

for any given reference trajectories satisfying the following assumption.

Assumption 4: The reference trajectory $x_d : \mathbb{R}_{\geq 0} \to \mathbb{R}$ is twice continuously differentiable and there exist positive constants B_{dp}, B_{dv}, and B_{da}, such that

$$|x_d(t)| \leq B_{dp}, \qquad |\dot{x}_d(t)| \leq B_{dv}, \qquad |\ddot{x}_d(t)| \leq B_{da},$$

for all $t \geq 0$. □

III. Global trajectory tracking

A. Proposed adaptive controller

For a given bounded desired trajectory, as described in Assumption 4, consider the following control law:

$$\begin{aligned} u = &- \sigma_1 (K_1 \bar{x}) - \sigma_2 (K_2 \dot{\bar{x}}) + m\ddot{x}_d(t) + f_v \dot{x}_d(t) \\ &+ f_c \tanh(\beta \dot{x}_d(t)) + \alpha g(x), \end{aligned} \tag{4}$$

where K_1, $K_2 \in \mathbb{R}_+$ are, respectively, the proportional and derivative control gains, and $\sigma_i : \mathbb{R} \to \mathbb{R}$, $i \in \{1, 2\}$, are globally Lipschitz saturation functions; they are strictly increasing, $\sigma_i(s)s > 0$ for all $s \neq 0$, $\sigma_i(0) = 0$, and there exists $M > 0$, such that $|\sigma(s)| \leq M$ for all $s \in \mathbb{R}$.

In the presence of loss of effectiveness, *i.e.,* if $\tau = \Delta(t)u$, Eq. (4) can be rewritten using Property 1 as

$$\begin{aligned} \Delta(t)u = &- \Delta(t)\sigma_1 (K_1 \bar{x}) - \Delta(t)\sigma_2 (K_2 \dot{\bar{x}}) \\ &+ X(x, \dot{x}_d, \ddot{x}_d)\,\theta(t) \end{aligned} \tag{5}$$

where $\theta \in \mathbb{R}^4$ is $\theta^\top(t) = \begin{bmatrix}\theta_1(t) & \theta_2(t) & \theta_3(t) & \theta_4(t)\end{bmatrix}$, with $\theta_1(t) \triangleq \Delta(t)m$, $\theta_2(t) \triangleq \Delta(t)f_v$, $\theta_3(t) \triangleq \Delta(t)f_c$, $\theta_4(t) \triangleq \Delta(t)\alpha$, and $X(x, \dot{x}_d, \ddot{x}_d) = [\ddot{x}_d \quad \dot{x}_d \quad \tanh(\beta\dot{x}_d) \quad g(x)]$. Since θ is unknown due to the loss of effectiveness, an adaptive mechanism is introduced to estimate θ online. Let $\hat{\theta} \in \mathbb{R}^4$ denote the estimate of θ. The adaptive subsystem is given by:

$$\hat{\theta} = s_a(\hat{\phi}) \tag{6a}$$

$$\dot{\hat{\phi}} = -K_a X(x, \dot{x}_d, \ddot{x}_d)^\top \left[\dot{\bar{x}} + \varepsilon \sigma_1 (K_1 \bar{x})\right] \tag{6b}$$

where $s_a(x)^\top = \begin{bmatrix}\sigma_{a1}(x_1) & \sigma_{a2}(x_2) & \sigma_{a3}(x_3) & \sigma_{a4}(x_4)\end{bmatrix}$, with σ_{aj}, $j \in \{1, 2, 3, 4\}$ being saturation functions as described above, $K_a = \mathrm{diag}[k_{a1}, k_{a2}, k_{a3}, k_{a4}] \in \mathbb{R}^{4\times 4}$ with $k_{aj} > 0$ for all $j \in \{1, 2, 3, 4\}$, and ε as described below

$$\varepsilon \leq \min\left\{ \sqrt{\frac{m\delta_m}{K_1 \sigma'_{M1}}}, \frac{f_v}{mK_1\sigma'_{M1}}, \frac{4\delta_m f_v}{4m\delta_m K_1 \sigma'_{M1} + C_2^2} \right\}. \tag{7}$$

Proposition 1: The closed-loop system is uniformly globally stable (the origin is uniformly stable and the solutions are uniformly globally bounded) and the tracking errors $(\bar{x}, \dot{\bar{x}}) \to 0$ as $t \to \infty$, for all gains satisfying the condition in (7). Furthermore, the trajectories evolve without surpassing the actuator capacity. □

Proof: The proof is presented in two parts. First, input boundedness is established, followed by the demonstration of the closed-loop stability properties.

Bounded Input

Since $\Delta(t) \leq 1$ for all $t \geq 0$, the control input in the case of failure can be upper bounded as follows:

$$\begin{aligned} -\Delta(t)\sigma_1 (K_1 \bar{x}) - \Delta(t)\sigma_2 (K_2 \dot{\bar{x}}) + X(t, x, \dot{x}_d, \ddot{x}_d)\theta \\ \leq M_1 + M_2 + \|X(x, \dot{x}_d, \ddot{x}_d)\|\|\theta\| < T \end{aligned}$$

Choosing $x_d(t)$ and its derivatives such that

$$\|X(x, \dot{x}_d, \ddot{x}_d)\|\|\theta\| < T - M_1 - M_2,$$

by Eq. (3), the input is concluded to be upper bounded by a value lower than its saturation bound.

Stability analysis

Subtracting $m\ddot{x}_d + f_v \dot{x}_d + f_c \tanh(\beta\dot{x}_d) + \alpha g(x)$ to the right-hand side of eqs. (1) and (5), the closed-loop system takes the form:

$$\begin{aligned} m\ddot{\bar{x}} + f_v \dot{\bar{x}} + f_c \bar{\sigma}_T(\dot{\bar{x}}) = &- \Delta(t)\sigma_1 (K_1 \bar{x}) - \Delta(t)\sigma_2 (K_2 \dot{\bar{x}}) \\ &+ X(x, \dot{x}_d, \ddot{x}_d)^\top \bar{s}_a(\bar{\phi}) \end{aligned} \tag{8a}$$

$$\dot{\bar{\phi}} = -K_a X(x, \dot{x}_d, \ddot{x}_d)^\top \left[\dot{\bar{x}} + \varepsilon \sigma_1 (K_1 \bar{x})\right] \tag{8b}$$

with $\bar{\sigma}_T(\dot{\bar{x}}) \triangleq \tanh(\beta(\dot{\bar{x}} + \dot{x}_d)) - \tanh(\beta\dot{x}_d)$, $\bar{\phi} = \hat{\phi} - \phi^*$, and

$$\bar{s}_a = s_a(\bar{\phi} + \phi^*) - s_a(\phi^*) \tag{9}$$

with $\phi^* = [\phi_1^* \ \phi_2^* \ \phi_3^* \ \phi_4^*]^\top$ such that $\sigma_{ai}(\phi_i^*) = \theta_i \in \mathbb{R}$ since on the time interval $(t_k, t_{k+1}]$ every ϕ_i is constant, for $i \in \{1, \ldots, 4\}$; σ_{ai} and $\bar{\sigma}_T(\dot{\bar{x}})$ are strictly increasing.

Remark 1: Strictly speaking, Eq. (8b) is valid only for almost all t. This is because, since ϕ^* is piecewise constant and $\dot{\bar{\phi}} \triangleq \dot{\hat{\phi}} - \dot{\phi}^*$, where $\dot{\hat{\phi}}$ is defined in (6b) and $\dot{\phi}^*(t) = 0$ for almost all t. However, this does not affect the unicity and existence of Carathéodory solutions of (8). •

Next, we construct a Lyapunov function that is independent of any constant value $\delta \in [\delta_m, 1]$, that $\Delta(t)$ could possibly take, and therefore serves as a common Lyapunov function for all subsystems associated with different values of the loss of effectiveness parameter. Let

$$V_2(t, \bar{x}, \dot{\bar{x}}, \bar{\phi}) = V_1(t, \bar{x}, \dot{\bar{x}}) + \int_0^{\bar{\phi}} s_a^\top(r) K_a^{-1} dr, \tag{10}$$

where

$$V_1(t, \bar{x}, \dot{\bar{x}}) = \frac{1}{2} m \dot{\bar{x}}^2 + \varepsilon \sigma_1(K_1 \bar{x})\dot{\bar{x}} + \gamma \int_0^{\bar{x}} \sigma_1(K_1 r) dr, \tag{11}$$

with $\varepsilon > 0$ complying with inequality (7), $\gamma \in (\delta_m, \varepsilon + \delta_m)$, and

$$\int_{0_4}^{\bar{\phi}} s_a^\top(r) K_a^{-1} dr = \sum_{i=1}^{4} \int_0^{\bar{\phi}_i} \bar{\sigma}_{ai}(r_i) k_{ai}^{-1} dr_i. \tag{12}$$

In view of the fact that the function on the right-hand side of (12) is locally quadratic, for V_2 we have

$$\begin{aligned} W_L(\bar{x}, \dot{\bar{x}}) + \int_0^{\bar{\phi}} s_a^\top(r) K_a^{-1} dr \leq V_2(t, \bar{x}, \dot{\bar{x}}, \bar{\phi}) \leq \\ W_U(\bar{x}, \dot{\bar{x}}) + \int_0^{\bar{\phi}} s_a^\top(r) K_a^{-1} dr \end{aligned} \tag{13}$$

$$W_L(\bar{x},\dot{\bar{x}}) \triangleq \frac{1}{2}\begin{bmatrix}\sigma_1(K_1\bar{x})\\ \dot{\bar{x}}\end{bmatrix}^\top \begin{bmatrix}\frac{\gamma}{K_1\sigma'_{M1}} & -\varepsilon\\ -\varepsilon & m\end{bmatrix}\begin{bmatrix}\sigma_1(K_1\bar{x})\\ \dot{\bar{x}}\end{bmatrix}$$

$$W_U(\bar{x},\dot{\bar{x}}) \triangleq \frac{1}{2}\begin{bmatrix}\bar{x}\\ \dot{\bar{x}}\end{bmatrix}^\top \begin{bmatrix}\gamma K_1\sigma'_{M1} & -\varepsilon K_1\sigma'_{M1}\\ -\varepsilon K_1\sigma'_{M1} & m\end{bmatrix}\begin{bmatrix}\bar{x}\\ \dot{\bar{x}}\end{bmatrix}$$

for any ε in compliance with Eq. (7) and $\gamma \in (\delta_m, \varepsilon+\delta_m)$. Moreover, W_L and W_U are positive definite and radially unbounded, since so is the function on the right-hand side of (12). Thus, the Lyapunov function V_2 is positive definite and radially unbounded.

On the other hand, the derivative of V_2 in (10), along the trajectories of the system (8) yields, for almost all t,

$$\begin{aligned}
&\dot{V}_2(t,\bar{x},\dot{\bar{x}},\bar{\phi})\\
&\quad= \dot{\bar{x}}\Big[-\Delta\sigma_1(K_1\bar{x}) - \Delta\sigma_2(K_2\dot{\bar{x}}) - f_v\dot{\bar{x}} - f_c\bar{\sigma}_T(\dot{\bar{x}})\Big]\\
&\qquad + \dot{\bar{x}}X(x,\dot{x}_d,\ddot{x}_d)^\top\bar{s}_a(\bar{\phi}) + \gamma\sigma_1(K_1\bar{x})\dot{\bar{x}}\\
&\qquad + \varepsilon\sigma_1(K_1\bar{x})\Big[-\Delta\sigma_1(K_1\bar{x}) - \Delta\sigma_2(K_2\dot{\bar{x}}) - f_v\dot{\bar{x}}\\
&\qquad - f_c\bar{\sigma}_T(\dot{\bar{x}})\Big] + \varepsilon\sigma_1(K_1\bar{x})X(x,\dot{x}_d,\ddot{x}_d)^\top\bar{s}_a(\bar{\phi})\\
&\qquad + \varepsilon m\sigma'_1(K_1\bar{x})K_1\dot{\bar{x}}^2\\
&\qquad - \bar{s}_a^\top(\bar{\phi})X\big(x,\dot{x}_d,\ddot{x}_d\big)^\top\left[\dot{\bar{x}}+\varepsilon\sigma_1(K_1\bar{x})\right]\\
&\quad= -\Delta\dot{\bar{x}}\sigma_2(K_2\dot{\bar{x}}) - \dot{\bar{x}}f_c\bar{\sigma}_T(\dot{\bar{x}}) - f_v\dot{\bar{x}}^2 - \varepsilon\Delta\sigma_1(K_1\bar{x})^2\\
&\qquad - \varepsilon f_v\sigma_1(K_1\bar{x})\dot{\bar{x}} - \varepsilon\Delta\sigma_1(K_1\bar{x})\sigma_2(K_2\dot{\bar{x}})\\
&\qquad - \varepsilon f_c\sigma_1(K_1\bar{x})\bar{\sigma}_T(\dot{\bar{x}}) + \varepsilon m\sigma'_1(K_1\bar{x})K_1\dot{\bar{x}}^2\\
&\qquad + (\gamma-\Delta)\sigma_1(K_1\bar{x})\dot{\bar{x}}.
\end{aligned}$$

Since $\Delta(t) \in [\delta_m, 1]$ for all $t \geq 0$ and all the saturation functions are globally Lipschitz and zero at zero, the right hand side of the last equation above may be upper bounded as

$$\begin{aligned}
\dot{V}_2(t,\bar{x},\dot{\bar{x}},\bar{\phi}) \leq\; & -\delta_m\dot{\bar{x}}\sigma_2(K_2\dot{\bar{x}}) - \dot{\bar{x}}f_c\bar{\sigma}_T(\dot{\bar{x}}) - f_v\dot{\bar{x}}^2\\
& - \varepsilon\delta_m\sigma_1(K_1\bar{x})^2 + \varepsilon\sigma'_{2M}K_2|\sigma_1(K_1\bar{x})||\dot{\bar{x}}|\\
& + \varepsilon f_c\beta\bar{\sigma}'_T|\sigma_1(K_1\bar{x})||\dot{\bar{x}}| + \varepsilon f_v|\sigma_1(K_1\bar{x})||\dot{\bar{x}}|\\
& + \varepsilon m\sigma'_{1M}K_1\dot{\bar{x}}^2 + \varepsilon|\sigma_1(K_1\bar{x})||\dot{\bar{x}}|.
\end{aligned}$$

In turn, we have

$$\begin{aligned}
\dot{V}_2(t,\bar{x},\dot{\bar{x}},\bar{\phi}) \leq & -\delta_m\dot{\bar{x}}\sigma_2(K_2\dot{\bar{x}}) - \dot{\bar{x}}f_c\bar{\sigma}_T(\dot{\bar{x}})\\
& - \begin{bmatrix}|\sigma_1(K_1\bar{x})|\\ |\dot{\bar{x}}|\end{bmatrix} W_{D2}(\bar{x},\dot{\bar{x}})\begin{bmatrix}|\sigma_1(K_1\bar{x})|\\ |\dot{\bar{x}}|\end{bmatrix},
\end{aligned}$$

where

$$W_{D2}(\bar{x},\dot{\bar{x}}) = \begin{bmatrix}\varepsilon\delta_m & -\frac{1}{2}\varepsilon C_2\\ -\frac{1}{2}\varepsilon C_2 & f_v - \varepsilon mK_1\sigma'_{1M}\end{bmatrix}$$

and $C_2 \triangleq K_2\sigma'_{2M} + f_c\beta\sigma'_{TM} + f_v + 1$.

It follows from (7) that $W_{D2}(\bar{x},\dot{\bar{x}})$ is positive definite. Therefore, we conclude that $\dot{V}_2(t,\bar{x},\dot{x},\bar{\phi}) \leq 0$, $\forall(t,\bar{x},\dot{\bar{x}},\bar{\phi}) \in \mathbb{R}_+\times\mathbb{R}\times\mathbb{R}\times\mathbb{R}^4$, with $\dot{V}_2(t,\bar{x},\dot{\bar{x}},\bar{\phi}) = 0$ holding if and only if $(\bar{x},\dot{\bar{x}}) = (0,0)$. As a result, the trivial solution $(\bar{x},\bar{\phi}) \equiv (0,0)$ is shown to be uniformly stable [21, Theorem 4.8]. Moreover, the fact that $\dot{V}_2(t,\bar{x},\dot{x},\bar{\phi}) \leq 0$ and V_2 is positive definite and radially unbounded, implies the uniform global boundedness of all the solutions. That is, the origin is uniformly globally stable [22]. Furthermore, integrating on both sides of (14) along the trajectories, from $t_\circ$ to ∞, for any $t_\circ \geq 0$, we obtain that $\sigma_1(K_1\bar{x})$, $\dot{\bar{x}} \in \mathcal{L}_2$. Since, in turn, $\widehat{\sigma_1(K_1\bar{x})}$, $\ddot{\bar{x}} \in \mathcal{L}_\infty$, it follows, from [23, Theorem 4.3.1], that

$$\lim_{t\to\infty}\sigma_1\big(K_1\bar{x}(t)\big) = \lim_{t\to\infty}\dot{\bar{x}}(t) = 0.$$

In view of the properties of σ_1 it follows that $\bar{x}(t) \to 0$ too. The result follows. ■

IV. Simulations

Two different dynamic models were used to evaluate the performance of the developed adaptive control. The first simulation example aims to show the performance on a system were the restorative force term is not present, depending only on friction forces to dissipate energy. The second, is a comparison against an adaptive controller designed for robot manipulators explicitly taking into account viscous and Coulomb friction. A 1-dof manipulator is considered and hence, the restorative force term takes the form $\alpha\sin(x)$.

A. Example 1

The first example was carried out using the dynamics of an asynchronous motor gearbox [24]. The system can be represented by eq. (1), whose parameters are listed in Table I, and the maximum allowed torque is 9.5 N·m.

TABLE I

Gearbox parameters

Parameter	Value	Units
m	$13\times10^{\ 4}$	kg·m^2
f_v	$17\times10^{\ 4}$	N·m·s/rad
f_c	0.478	N·m
β	$10.78\times10^{\ 4}$	
α	0	

The simulation also accounts for unknown parametric values. The saturation functions involved in the control law Eqs. (5) and (6) were chosen as follows:

$$\sigma_1(K_1\bar{x}) = 5\tanh(K_1\bar{x}) \quad \sigma_2(K_2\dot{\bar{x}}) = 2\tanh(K_2\dot{\bar{x}})$$
$$\sigma_{aj}(x_j) = 2\tanh(x_j) \quad \sigma_{a4}(x_4) = 0\tanh(x_4)$$

with $j \in \{1,2,3\}$. The loss of efficiency is defined as

$$\Delta(t) = \begin{cases}1, & t < 30,\\ 0.7, & 30 \leq t < 70,\\ 1, & t \geq 70\end{cases} \tag{14}$$

the gain matrix $K_a = \mathrm{diag}[20, 15, 20, 0]$, $\varepsilon = 0.25$[1], $K_1 = 75$, $K_2 = 0.1$, and $x_d(t) = \frac{\pi}{4} + \sin\left(\frac{\pi}{4}t\right)$. The initial conditions were set to $x(0) = 0$ $\dot{x}(0) = 0$.

The results are shown in Figs. 1 and 2, the angle position error is shown in Fig. 1; observe that the error is small, and that when the input failure occurs from $t = 30$s to $t = 70$s, the performance is maintained. The computed control input

[1]The value of ε considered here, exceeds that obtained from Eq. (7). Nevertheless, this bound corresponds to a worst-case scenario; therefore larger value may still guarantee uniformly stability.

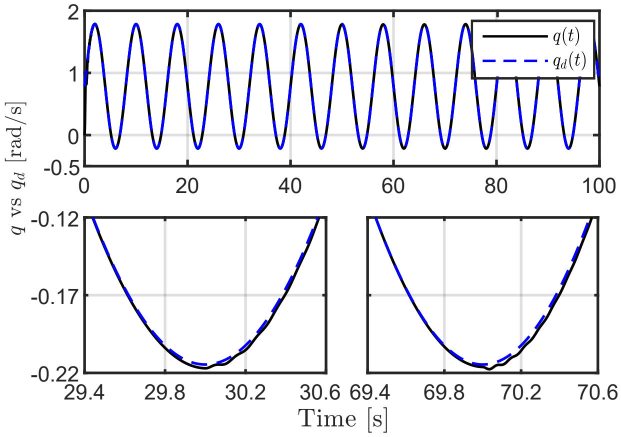

Fig. 1. Position error

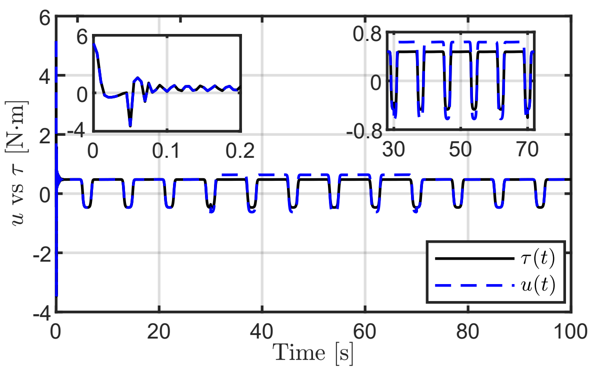

Fig. 2. Computed input versus actuator output

u is shown alongside the output from the faulty actuator in Fig. 2. It can be observed that, in order to maintain an output torque level τ capable of driving the trajectory tracking error to zero, the calculated control input u must increase when the loss of effectiveness occurs. Notice in the small inset figure that the signal never reaches the saturation limit.

Example 2

For comparison purposes, the control law proposed by [12], in the following referred to as $Z00$, was implemented using the *Pendubot* platform designed and identified in [25] configured as a single pendulum. The dynamics are given by

$$mL^2\ddot{x} + f_v\dot{x} + f_c\tanh(\beta\dot{x}) + mgL\sin(x) = \tau$$

where $m = 0.55$kg, $L = 0.3$m, $f_v = 0.093$N·m , $f_c = 0.01$, $\beta = 1$ and $g = 9.81$ kg·m/s^2.

The controller Z00 was designed for robot manipulators with *parametric uncertainties*; however, the considered dynamics account for static and dynamic friction terms. The control law, for a 1-dof manipulator, has the form:

$$\tau = Y\hat{\phi} - K_1\tanh(\bar{x}) - K_2\tanh(\dot{x}) \tag{15a}$$

$$\dot{\hat{\phi}} = \mathrm{proj}(\Omega) \tag{15b}$$

$$\Omega = -K_a Y(x,\dot{x})\left(\dot{x} + \varepsilon\tanh(\bar{x})\right) \tag{15c}$$

where K_1, K_2, K_a and ε are positive constants, the projection function as defined in [12], and $\hat{\phi}$ representing the approximation of the unknown f_c. For the SP-SD algorithm the saturation functions are the same as in Experiment 1. The design parameters shown in Table II were selected to perform the simulation. The control gains were empirically adjusted to achieve the best response for each control algorithm, we set

$$\Delta(t) = \begin{cases} 1, & t < 10, \\ 0.5, & 10 \le t < 30, \\ 0.8, & 30 \le t < 40, \\ 1, & t \ge 40 \end{cases} \tag{16}$$

TABLE II

DESIGN PARAMETERS

Parameter	Z00	SP-SD
x_d	$\sin\left(\frac{2\pi}{3}t\right) + \pi/2$	$\sin\left(\frac{2\pi}{3}t\right) + \pi/2$
$x(0)$	0	0
K_1	30	15
K_2	3	5
K_a	20	diag{6.5 , 10 , 8 , 5}
ε	0.5	0.38

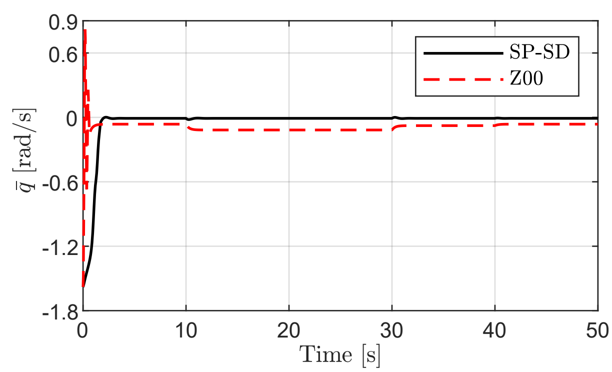

Fig. 3. Position error

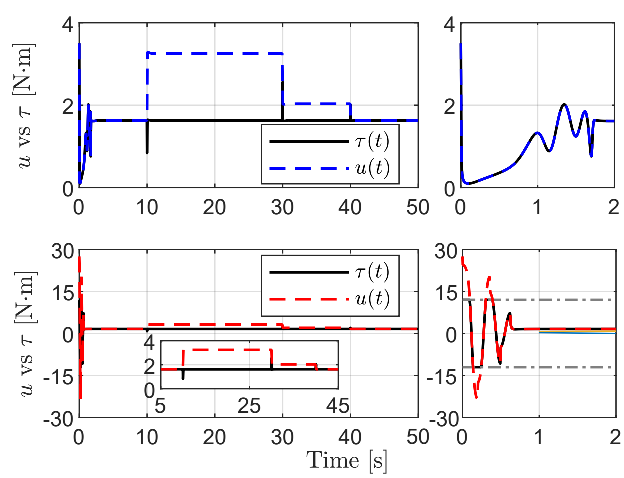

Fig. 4. Computed input versus actuator output

As shown in Figure 3, both algorithms make the positions stay close to the desired trajectory. However, the proposed algorithm results in smaller errors and provides a smoother response. Figure 4 compares the commanded input $\tau(t)$ with the actual input delivered $u(t)$, for the SP-SD and Z00 algorithms. The small figures on the right show the first seconds of the inputs, observe that the Z00 algorithm reaches saturation, while the proposed algorithm operates within the actuator saturation limit (± 12 Nm).

V. Conclusions

An adaptive algorithm was introduced to accurately track a desired trajectory in the presence of loss of efficiency affecting the input, while explicitly taking into account the actuator natural saturation limits. The control scheme compensates for dry friction by employing a friction model formulated with an hyperbolic tangent function. To illustrate the efficacy of the proposed adaptive control law, simulations with different mechanical systems were conducted, demonstrating robust performance under varying conditions and confirming the system ability to sustain stability and achieve the desired tracking objectives despite frictional and saturation effects. Current work is devoted to extending these preliminary results to handle additional uncertainties in systems of higher order.

Acknowledgment

We would like to express our gratitude to our dear friend and colleague Jesus Sosa, whose invaluable insights and contributions during the initial planning of this article were pivotal. Although he is no longer with us, his memory and intellectual legacy continue to inspire our work. This article is dedicated to him.

The first author gratefully acknowledges the *Laboratoire des signaux et systèmes* for providing an excellent support and research environment during the sabbatical stay.
The results presented here belong to the projects I×M SECIHTI no. 621 and 843.

References

[1] Q. Wang, Y. Yang, H. Fang, and Y. Wan, "Input saturation: academic insights and future trends," *International Journal of Systems Science*, vol. 53, no. 6, pp. 1138–1152, 2022.

[2] J. C. Maré, "Practical considerations in the modelling and simulation of electromechanical actuators," *Actuators*, vol. 9, no. 4, p. 94, 2020.

[3] P. C. Berri, M. D. L. Dalla Vedova, and P. Maggiore, "A smart electromechanical actuator monitor for new model-based prognostic algorithms," *International Journal of Mechanics and Control*, vol. 17, no. 2, pp. 19–25, 2016.

[4] X. C. Wang, B. Huang, R. L. Wang, J. L. Mo, and H. Ouyang, "Friction-induced stick-slip vibration and its experimental validation," *Mechanical Systems and Signal Processing*, vol. 142, p. 106705, 2020.

[5] T. Kheowree and S. Kuntanapreeda, "Adaptive dynamic surface control of an electrohydraulic actuator with friction compensation," *Asian Journal of Control*, vol. 17, no. 3, pp. 855–867, 2015.

[6] W. Ruan, Q. Dong, X. Zhang, and Z. Li, "Friction compensation control of electromechanical actuator based on neural network adaptive sliding mode," *Sensors*, vol. 21, no. 4, p. 1508, 2021.

[7] C. Makkar, W. E. Dixon, W. G. Sawyer, and G. Hu, "A new continuously differentiable friction model for control systems design," in *Proceedings of the IEEE/ASME International Conference on Advanced Intelligent Mechatronics*, Monterey, USA, 2005, pp. 600–605.

[8] C. Makkar, G. Hu, W. G. Sawyer, and W. E. Dixon, "Lyapunov-based tracking control in the presence of uncertain nonlinear parameterizable friction," *IEEE Transactions on Automatic Control*, vol. 52, no. 10, pp. 1988–1994, 2007.

[9] J. Na, Q. Chen, X. Ren, and Y. Guo, "Adaptive prescribed performance motion control of servo mechanisms with friction compensation," *IEEE Transactions on Industrial Electronics*, vol. 61, no. 1, pp. 486–494, 2013.

[10] S. Wang and J. Na, "Parameter estimation and adaptive control for servo mechanisms with friction compensation," *IEEE Transactions on Industrial Informatics*, vol. 16, no. 11, pp. 6816–6825, 2020.

[11] W. E. Dixon, "Adaptive regulation of amplitude limited robot manipulators with uncertain kinematics and dynamics," *IEEE Transactions on Automatic Control*, vol. 52, no. 3, pp. 488–493, 2007.

[12] E. Zergeroglu, W. Dixon, A. Behal, and D. Dawson, "Adaptive setpoint control of robotic manipulators with amplitude-limited control inputs," *Robotica*, vol. 18, no. 2, pp. 171–181, 2000.

[13] C. Guan and S. Pan, "Nonlinear adaptive robust control of single-rod electro-hydraulic actuator with unknown nonlinear parameters," *IEEE Transactions on Control Systems Technology*, vol. 16, no. 3, pp. 434–445, 2008.

[14] Y. Tang, Z. Zhu, G. Shen, G. Rui, D. Cheng, X. Li, and Y. Sa, "Real-time nonlinear adaptive force tracking control strategy for electrohydraulic systems with suppression of external vibration disturbance," *Journal of the Brazilian Society of Mechanical Sciences and Engineering*, vol. 41, pp. 1–16, 2019.

[15] D. J. López-Araujo, A. Zavala-Río, V. Santibáñez, and F. Reyes, "A generalized global adaptive tracking control scheme for robot manipulators with bounded inputs," *International Journal of Adaptive Control and Signal Processing*, vol. 29, no. 2, pp. 180–200, 2015.

[16] J. L. Serres, D. B. Reynolds, C. A. Phillips, M. J. Gerschutz, and D. W. Repperger, "Characterisation of a phenomenological model for commercial pneumatic muscle actuators," *Computer Methods in Biomechanics and Biomedical Engineering*, vol. 12, no. 4, pp. 423–430, 2009.

[17] H. J. M. T. S. Adriaens, W. L. De Koning, and R. Banning, "Modeling piezoelectric actuators," *IEEE/ASME Transactions on Mechatronics*, vol. 5, no. 4, pp. 331–341, 2000.

[18] N. Mostaghel, "A non-standard analysis approach to systems involving friction," *Journal of Sound and Vibration*, vol. 284, no. 3–5, pp. 583–595, 2005.

[19] E. Pennestri, V. Rossi, P. Salvini, and P. P. Valentini, "Review and comparison of dry friction force models," *Nonlinear Dynamics*, vol. 83, pp. 1785–1801, 2016.

[20] L. Zhang, W. Chen, J. Liu, and C. Wen, "A robust adaptive iterative learning control for trajectory tracking of permanent-magnet spherical actuator," *IEEE Transactions on Industrial Electronics*, vol. 63, no. 1, pp. 291–301, 2015.

[21] H. Khalil, *Nonlinear Systems*, 3rd ed. Upper Saddle River, NJ: Prentice Hall, 2002.

[22] M. Krstić, I. Kanellakopoulos, and P. Kokotović, *Nonlinear and Adaptive control design*. New York: John Wiley & Sons, Inc., 1995.

[23] P. A. Ioannou and J. Sun, *Adaptive Control*. Mineola, NY: Dover Publications, 2012.

[24] C. Roldán, F. J. Campa, O. Altuzarra, and E. Amezua, "Automatic identification of the inertia and friction of an electromechanical actuator," in *New Advances in Mechanisms, Transmissions and Applications*. Dordrecht: Springer, 2014, pp. 409–416.

[25] F. Wiebe, S. Kumar, L. J. Shala, S. Vyas, M. Javadi, and F. Kirchner, "Open source dual-purpose acrobot and pendubot platform: Benchmarking control algorithms for underactuated robotics," *IEEE Robotics & Automation Magazine*, vol. 31, no. 2, pp. 113–124, 2023.